the FEBS Journal

On the mechanisms of glycolytic oscillations in yeast

Mads F. Madsen[1], Sune Danø[2] and Preben G. Sørensen[1]

1 Functional Dynamics Group, Department of Chemistry, University of Copenhagen, Denmark
2 Department of Medical Biochemistry and Genetics, University of Copenhagen, Denmark

Keywords
glycolysis; Hopf bifurcation; metabolic control analysis; oscillations; oscillophore

Correspondence
S. Danø, Department of Medical Biochemistry and Genetics, University of Copenhagen, Blegdamsvej 3b, 2200 Copenhagen N, Denmark
Fax: +45 35 35 63 10
Tel: +45 35 32 77 53
E-mail: sdd@kiku.dk

(Received 6 October 2004, revised 28 February 2005, accepted 2 March 2005)

doi:10.1111/j.1742-4658.2005.04639.x

This work concerns the cause of glycolytic oscillations in yeast. We analyse experimental data as well as models in two distinct cases: the relaxation-like oscillations seen in yeast extracts, and the sinusoidal Hopf oscillations seen in intact yeast cells. In the case of yeast extracts, we use flux-change plots and model analyses to establish that the oscillations are driven by on/off switching of phosphofructokinase. In the case of intact yeast cells, we find that the instability leading to the appearance of oscillations is caused by the stoichiometry of the ATP-ADP-AMP system and the allosteric regulation of phosphofructokinase, whereas frequency control is distributed over the reaction network. Notably, the NAD^+/NADH ratio modulates the frequency of the oscillations without affecting the instability. This is important for understanding the mutual synchronization of oscillations in the individual yeast cells, as synchronization is believed to occur via acetaldehyde, which in turn affects the frequency of oscillations by changing this ratio.

Autonomous oscillations in the concentrations of glycolytic intermediates reflect the dynamics of control and regulation of this major catabolic pathway, and the phenomenon has been reported in a broad range of cell types [1–6]. Understanding glycolytic oscillations might therefore prove crucial for our general understanding of the regulation of metabolism and the interplay among different parts of metabolism as illustrated by the hypothesis that glycolytic oscillations play a role in complex pulsatile insulin secretion [7]. The key question in this context is the mechanism(s) of the oscillations, but despite much work over the last 40 years it remains unsettled.

Here we address this question for the particular case of yeast. We focus on the yeast systems as these are particularly well studied; as such they can be seen as prototypes of glycolytic oscillations (recently reviewed in [8,9]). Our approach emphasizes the general dynamic properties of the oscillations. This leads us to analyse the cases of extracts and intact cells separately. With this starting point we can utilize our recently developed theoretical tools in the analyses [10]. The advantages are that more experimental data can be included in the analyses, and that these are carried out on a rigorous mathematical basis. In short, we answer two related questions in this work: 'what is the mechanism of glycolytic oscillations in yeast extracts?' and 'what is the mechanism of glycolytic oscillations in intact yeast cells?'

Dynamic properties of glycolytic oscillations

Glycolytic oscillations are recorded as time traces of NADH fluorescence [11]. Yeast extracts readily exhibit oscillations, either upon administration of trehalose,

Abbreviations
ACA, acetaldehyde; ADH, alcohol dehydrogenase; AK, adenylate kinase; ALD, aldolase; CSTR, continuous-flow stirred tank reactor; DHAP, dihydroxyacetone phosphate; F6P, fructose 6-phosphate; FBP, fructose 1,6-bisphosphate; G6P, glucose 6-phosphate; GAP, glyceraldehyde 3-phosphate; GAPDH, glyceraldehyde-3-phosphate dehydrogenase; HK, hexokinase; PFK, phosphofructokinase-1; PGI, phosphoglucoisomerase; PK, pyruvate kinase; Pyr, pyruvate; TIM, triosephosphate isomerase.

which is slowly degraded to glucose, or when fed with a constant inflow of glucose or fructose. The generic type of oscillations in yeast extracts is relaxation oscillations, i.e. the cycle is composed of short time intervals where the NADH level changes fast, and long time intervals with slow changes (Fig. 2, [12]) for a typical example. Other types of oscillations have also been observed, e.g. sinusoidal, period-doubled or chaotic oscillations [13,14], but these are rare special cases. Therefore, we focus on relaxation-like oscillations for the case of yeast extracts. From the point of view of nonlinear dynamics, such oscillations indicate that the system is composed of processes taking place on distinct fast and slow time-scales. It is sometimes – but not always – possible to identify these separate processes in mechanistic terms: in the case of a dripping water tap, the slow time-scale corresponds to the growing droplet, and the fast time-scale corresponds to the actual drip of the drop. In the case of yeast extracts, we will show below that the slow time-scale corresponds to removal of the allosteric phosphofructokinase-1 (PFK) inhibitor ATP and/or build-up of its allosteric activator AMP and its substrate fructose 6-phosphate (F6P), whereas the fast time-scale corresponds to bursts of PFK activity.

The oscillations seen in suspensions of intact yeast cells have smaller relative amplitude than those seen in extracts, and the shape is almost sinusoidal. This holds for oscillations in single yeast cells as well [15]. Relaxation-like oscillations have never been observed. (The spiked oscillations reported in [16] is an artefact [17].)

In previous experimental work, we have characterized the oscillatory dynamics of yeast cell suspensions, and we found that the yeast cells behave according to the universal dynamics of systems close to a supercritical Hopf bifurcation [18]. In this context, universality means that the laws governing the time-evolution of any system in the neighbourhood of such a bifurcation are the same; system specificity is reflected by differences in parameters.

The physical basis for this universality is the separation of time-scales in the neighbourhood of bifurcations. For the supercritical Hopf bifurcation, these laws dictate that the unperturbed system moves on a small-amplitude limit cycle, which, essentially, is confined to a two-dimensional plane. Accordingly, the persistent behaviour of the system can be described by just two variables, which can be viewed as an activating and an inhibiting mode. We have shown experimentally that yeast cell suspensions behave according to these laws (Fig. 10 of [19]).

The two-dimensional plane of the limit cycle is embedded in the high-dimensional concentration space describing the state of the cell in terms of all relevant metabolite concentrations. Despite the high dimension of concentration space, we show below that, in the specific case of glycolytic oscillations in intact yeast cells, it is possible to identify these two Hopf modes with two small sets of metabolites.

Proposed mechanisms of glycolytic oscillations

The emergence and properties of glycolytic oscillations have been discussed previously along four major lines: (a) allosteric control of PFK; (b) distributed control of oscillations; (c) hexose transport kinetics and (d) ATP autocatalysis due to the stoichiometry of glycolysis.

PFK kinetics

In early analyses, PFK with its allosteric regulation [in particular substrate inhibition by ATP and product activation by AMP and fructose 1,6-bisphosphate (FBP)] was pointed out as the source of the oscillations and termed 'the oscillophore' [1,20]. The analysis of these early observations, as well as a substantial amount of additional experimental evidence supporting the conclusion, is summarized in section 2.1 of [21] (see also [22–25]). The basis for this conclusion is a special application of the crossover theorem [26], where enzymatic control points of oscillatory glycolysis are identified as being those enzymes with the largest phase-shift between substrates and products. From a contemporary point of view, the theoretical motivation for the application of the crossover theorem in the analysis of glycolytic oscillations is weak [27].

Another argument in favour of the PFK hypothesis is the fact that yeast extracts fed with the PFK substrate F6P can show oscillations, whereas oscillations have not been observed when extracts are fed with the PFK product FBP. While this shows that PFK is indeed important for glycolytic dynamics, it is not in itself a proof that PFK is the primary cause of the oscillations. It should be emphasized, though, that the well-known allosteric regulations of PFK do provide a mechanism by which its postulated role as oscillophore can be explained [20,28,29].

Distributed control

One could expect that oscillations, fluxes and concentrations are systemic properties determined by the interplay between the constituents of the biochemical system. Hence, PFK is probably not the only part of the network exerting control on its dynamic properties.

Based on the phase angles of the glycolytic intermediates in yeast extracts, Boiteux and Hess point to pyruvate kinase (PK) and the enzyme pair phosphoglycerate kinase and glyceraldehyde-3-phosphate dehydrogenase (GAPDH) as additional control points conveying the adenine nucleotide signal from PFK to other parts of the network [24]. As discussed below, hexose transport kinetics and the glycolytic ATP stoichiometry are also thought to be important in this context. More recently, the redox feedback loop constituted by the conserved sum of NAD^+ and NADH has received some attention as it plays a key role in the acetaldehyde (ACA) based mechanism believed to be responsible for the active synchronization of the oscillations among the individual yeast cells; ACA diffuses freely in and out of the cells. Here it acts as substrate for the alcohol dehydrogenase (ADH), producing ethanol and oxidizing NADH to NAD^+. The altered $NAD^+/NADH$ ratio then modulates the phase of the oscillations via the GAPDH reaction [30,31].

In an effort to quantify such considerations, Westerhoff and coworkers have applied metabolic control analysis (a form of sensitivity analysis) on a number of mathematical models of glycolytic oscillations. They conclude that the control of the oscillations is distributed throughout the network [32–34]. The implication is that the oscillations are a property of the entire network, and that one cannot dissect the network and identify the mechanism responsible for the oscillations. Note, however, that all but one of the models investigated in these studies are core models, which aim at describing the 'essential' parts of the glycolytic oscillator. Hence, it may not be that surprising that all components of these models are important for the dynamics.

Hexose transport

Becker and Betz point to the hexose transport step as an important control point of the oscillatory dynamics, but still suggest PFK as the primary source of the oscillations [35]. According to Reijenga *et al.*, hexose transport has 'most but not all' control of the dynamics [36]. The control coefficients determined in that study can, however, be positive as well as negative (e.g. Fig. 3b), so one cannot judge the importance of a single step from its control coefficient and a summation theorem. Still, their experiments emphasize and quantify the importance of hexose transport kinetics in the context of glycolytic oscillations.

The main role of hexose transport kinetics would be to set the rate of substrate inflow for glycolysis. Indeed, glucose transport is saturated in the experiment by Reijenga *et al.*, and the substrate inflow rate is known to be an important effector of the dynamics in yeast extracts [37].

Autocatalytic stoichiometry of ATP

The stoichiometry of glycolysis makes the pathway autocatalytic in ATP, as two moles of ATP per mole of glucose are consumed in the upper part of glycolysis, yielding four moles of ATP in the lower part. Indeed, Sel'kov and Aon *et al.* have proposed models for glycolytic oscillations based entirely on this mechanism [38,39]. This is, however, not generally considered the primary cause of glycolytic oscillations.

Results

Intact yeast cells: Hopf dynamics

Phase plane analysis of experimental data

Two complete experimental data sets on phases and amplitudes of glycolytic metabolite oscillations in intact yeast cells exist in the literature. When analysed by means of polar phase plane plots, such data can provide a biochemical interpretation of the underlying dynamical structures. The analysis is briefly described in Materials and methods.

In the study of Betz and Chance samples were removed with a 5–6 s interval from a suspension of glucose consuming *Saccharomyces carlsbergensis* which showed damped oscillations upon the transition from aerobic to anaerobic conditions [40]. The fluorescence signal reflecting the NADH concentration was measured simultaneously. Data is available on the amplitudes and phases of ATP, ADP, AMP, glucose 6-phosphate (G6P), F6P, FBP, dihydroxyacetone phosphate (DHAP), glyceraldehyde 3-phosphate (GAP) and pyruvate (Pyr). The sampling covers the very first one and a half cycles of oscillations emerging after the transition to anaerobic conditions.

In the data set from *Saccharomyces cerevisiae* reported by Richard *et al.*, sampling was performed in such a way that the initial transients following first glucose addition ($t = 0$ min) and subsequently cyanide addition ($t = 4$ min) had died out and the yeast cells exhibited stable oscillations [41]. (Typically, sampling was performed from $t = 9$ min to $t = 11$ min with a sampling interval of 5 s.) Amplitudes and relative phases were determined for G6P, F6P, FBP, ATP, ADP, AMP, NADH, NAD^+, extracellular ACA and inorganic phosphate. The phosphate measurements,

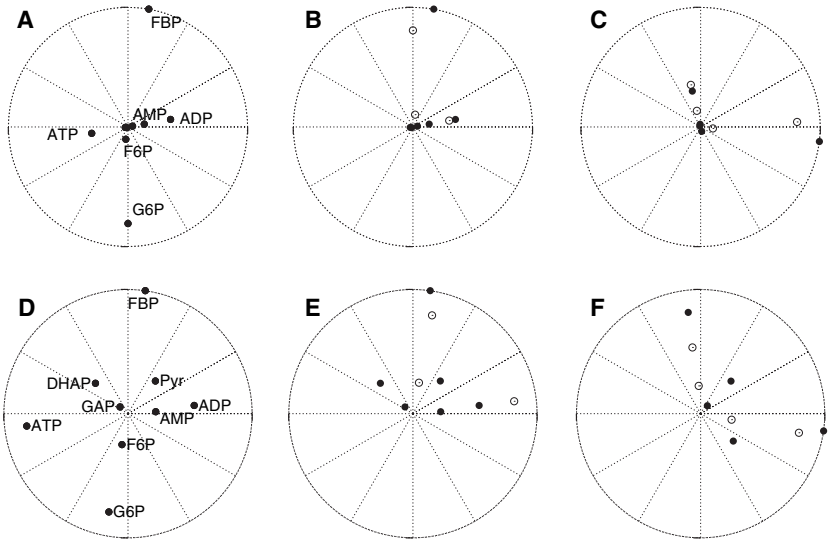

Fig. 1. Experimental polar phase plane plots. (A–C) Data from [41]. (D–F) Data from [40]. A and D are the relative phases and amplitudes plotted with annotations showing the major components. Apart from these, A also contains data on NAD^+, NADH and extracellular ACA, which all have very low amplitudes. In the remaining four panels, some metabolite phases have been flipped 180°, now indicating the relative phases of the minima instead of the maxima of their oscillations. This is shown by a ○ in the plots. (G6P, F6P and ATP have been flipped in B and E, and in C and F, AMP, ADP, G6P and F6P have been flipped.) The rotation of the plots are the same in panels A, B, D, and E, whereas panels C and F have been rotated 90° clockwise. All amplitudes are relative to the FBP amplitude. See text for discussion and interpretation.

however, have not been included in our analysis as they were made at 20 °C, whereas all other experiments were performed at 25 °C. Measurements of fructose 2,6-bisphosphate, DHAP, GAP, 1,3-bisphosphoglycerate, 3-phosphoglycerate, 2-phosphoglycerate, phosphoenolpyruvate and Pyr were also performed, but these metabolites did not show clear oscillations.

The polar phase plane plots of these two data sets are shown in Fig. 1. Panels A–C are taken from [41] and the remaining three panels show the data from [40]. The data points are annotated in A and D, and the two panel pairs B,E and C,F show two different representations of the same data. In B, an $\approx 90°$ structure is evident. As explained in Materials and methods, this structure indicates that the system can be described in terms of two interacting modes. The first mode activates the second, and the second inhibits the first. The activating mode is the abundance of AMP and ADP, and scarcity of ATP (i.e. the minimum of the ATP oscillation instead of the maximum), and the inhibitory mode is abundance of FBP and scarcity of G6P and F6P.

Biochemically, the activating mode corresponds to low energy charge, and the inhibitory mode is high levels of substrate for the lower part of glycolysis and low levels for the upper part. The activation of this mode by low energy charge can be explained as activation of PFK and inhibition of hexokinase (HK). The inhibitory feedback is a consequence of the glycolytic stoichiometry, where ATP is consumed in the upper part of glycolysis and produced in the lower part. Accordingly, the energy charge is increased when the flux is increased in the lower part of glycolysis and decreased in the upper.

The same phase plane structure is found in the data set from Betz and Chance (panel E) [40], but an additional system involving DHAP and Pyr is seen as well, and the ATP amplitude is markedly larger. Thus, the oscillations seen in this experiment cannot be explained solely in terms of PFK kinetics and the ATP-ADP-AMP system. A possible explanation for this discrepancy is the fact that the data from [40] were collected immediately after the transition from aerobic to anaerobic metabolism. This is a large perturbation of the cellular redox state, and DHAP and Pyr are located at branch points in the reaction network where the flux through the branches depend on the availability of NADH (for the glycerol 3-phosphate dehydrogenase reaction in the case of DHAP and for the ADH reaction in the case of Pyr).

C and F show another possible interpretation of the data; in this case the activating mode is abundance of FBP and scarcity of G6P and F6P, and the inhibiting mode is high energy charge. The activating and inhibiting feedback can be explained by the same reasoning as given for the interpretation in panels B and E; the

comments regarding DHAP and Pyr in the dataset from [40] apply equally well. This holds for other possible interpretations as well.

To conclude, we note that the 90° structure of the universal Hopf dynamics is reflected in the biochemical phase plane plot with a limited number of components in each of the two modes. In particular, this holds for the data set from yeast cells showing stable oscillations where initial transients have died out [41]. The biochemical interactions among these modes can be explained in terms of the known allosteric regulation of PFK, and the ATP-ADP-AMP stoichiometry of the glycolytic system.

Analysis of a model describing oscillations in intact cells

Our full-scale model of glycolysis was developed with the intention of reproducing as many experimental findings as possible [19]. In particular, the model shows oscillations and possesses a supercritical Hopf bifurcation. The model is analysed in the form described in [19].

Figure 2 shows a polar phase plane plot of this model at the supercritical Hopf bifurcation found at a mixed flow glucose concentration of 18.5 mM [19]. The G6P phase is not entirely correct in the model but the phase plane plot is similar to the experimental phase plane plots; in particular that obtained from yeast cells showing stable oscillations [41]. Figure 2B shows the same interpretation as in Fig. 1B,E, and the conclusion is the same: the oscillations can be understood largely in terms of two modes composed of a well-defined subset of metabolites, and the inhibition or activation among these two modes can be explained in terms of (a) PFK kinetics modelled by:

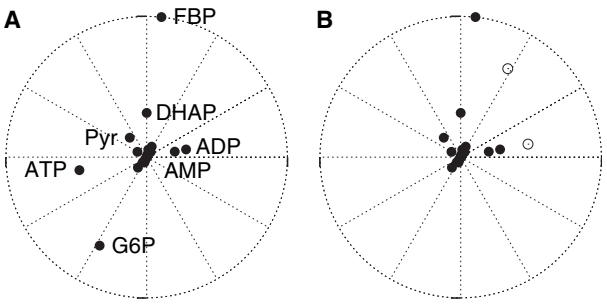

Fig. 2. Polar phase plane plots of the model by Hynne *et al.* [19]. (A) Annotations of the major components. (B) Interpretation of the data discussed in the text. In this panel, the phases of ATP and G6P have been flipped 180°, indicating the relative phases of the minima of their oscillations. This is shown by a ○ in the plot. The rotation of the plots are the same in the two panels, and amplitudes have been scaled such that FBP has full amplitude. Calculations are performed at the Hopf bifurcation described in [19]. See text for discussion.

$$\upsilon = \frac{V_{\max}[\mathrm{F6P}]^2}{K\left(1+\kappa\frac{[\mathrm{ATP}]^2}{[\mathrm{AMP}]^2}\right)+[\mathrm{F6P}]^2},$$

and (b) the ATP-ADP-AMP system and the network structure.

The results of the sensitivity analysis (Materials and methods) at super-critical Hopf bifurcations, i.e. calculations of $C_p^{\omega_{\mathrm{lc}}}$ (Eqn 3) and σ_p' (Eqn 4) in the same bifurcation point, is shown in Fig. 3.

Figure 3A shows that the stability of the stationary state is controlled by PFK and by the ATP-ADP-AMP system through its interactions with HK, glycogen formation and unspecific ATP consumption. PFK tends to make the system more unstable, whereas ATP consuming processes stabilize the system.

In contrast to this rather simple picture, Fig. 3B shows that several control systems affect the frequency

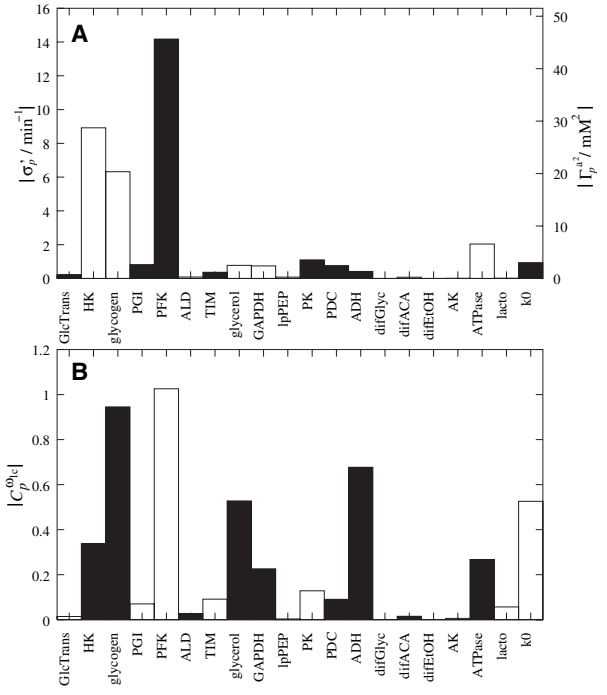

Fig. 3. Sensitivity analysis at the Hopf bifurcation of the model by Hynne *et al.* [19]. (A) Relative change of stability with $V_{\max}$ or mass-action rate constants for all reactions (Eqn 4). (B) Frequency control coefficients on the emerging limit cycle (Eqn 3). For reversible reactions, the coefficients for the forward and the reverse reactions are added in order to reflect the effect of increasing the enzyme concentration. Black bars represent positive values, and white bars represent negative. Calculations are performed at the Hopf bifurcation described in [19]. GlcTrans, glucose transporter; Glycogen, glycogen branch; glycerol, glycerol branch; lpPEP, lumped phosphoglycerate kinase, phosphoglycerate mutase, and enolase reactions; PDC, pyruvate decarboxylase; difGlyc, glycerol diffusion; difACA, ACA diffusion; difEtOH, ethanol diffusion; lacto, lactonitrile formation; k-^{0}, specific flow of the CSTR.

of oscillation. Equation 3 (Materials and methods) shows that frequency control is the sum of a σ'_p term and a σ''_p term. Therefore, it is generally expected that reactions with substantial control of stability (i.e. a numerically large σ'_p) will also control frequency. The remaining reactions with frequency control (i.e. those that have a numerically large σ''_p) are GAPDH, ADH, glycerol formation, and the specific flow of the continuous-flow stirred tank reactor (CSTR). Apart from the mechanical flow, these are all part of the NAD^+/NADH feedback system, so this control system affects the frequency of the oscillations without affecting the stability of the reaction system.

Yeast extracts: Relaxation dynamics

Estimation of flux changes from experimental data

In the analysis of relaxation-like oscillations, one is looking for separate processes being turned on and off on long and short time-scales. On/off switching can be revealed by plotting the ratio of the velocity change across a period relative to the minimum velocity within the oscillatory cycle as described in the Materials and methods section. Using amplitude and phase information from [12] and flux information from [22] we have assembled the experimental flux-change diagram shown in Fig. 4. It shows very large flux changes for phosphoglucoisomerase (PGI) and PFK as well as for the ATPase reaction also reported to be active in these yeast extracts. All other reactions show flux changes that are substantially smaller. This result is in good agreement with the PFK hypothesis for glycolytic oscillations. (The flux changes of PGI can be assumed driven by those of PFK.)

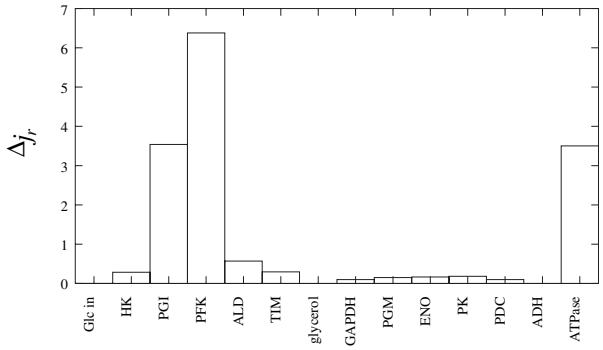

Fig. 4. Relative flux changes in yeast extract experiments. For each reaction, the flux change designates the ratio of the change of flux across a period relative to the minimum flux in the oscillatory cycle. Calculations are based on experimental amplitude and phase data from [12] and experimental flux data from [22]. Sinusoidal oscillations are assumed. Glc in, glucose inflow; glycerol, glycerol branch; PGM, phosphoglycerate mutase; ENO, enolase; PDC, pyruvate decarboxylase.

Comparison with the nine-variable model by Wolf et al.

The PFK hypothesis for yeast extracts is further substantiated by comparison with the model for glycolytic oscillations presented in [31]. (Here this model is analysed at the point defined by Table 1 of [31] with the additional condition $k_9 = 80\ \text{min}^{-1}$; this point is the same point as that analysed in [33].) Originally, this model was intended to model oscillations in intact yeast cells but, from the point of view of nonlinear dynamics, the model behaves more like oscillating yeast extracts; the oscillations are relaxation-like, and the model does not possess the supercritical Hopf bifurcation found in oscillating yeast cells (instead, a subcritical Hopf bifurcation is found at the onset of oscillations). Most importantly, the flux-change diagram in Fig. 5 shows good – although not quantitative – agreement with the diagram based on experimental data (Fig. 4). In this model the HK, PGI and PFK reactions are combined in one reaction; the large flux-change of the HK-PFK reaction corresponds to the large PGI flux change and the even larger PFK flux change seen experimentally.

The HK-PFK reaction is modelled by the highly nonlinear kinetics

$$v = k_1, \frac{[\text{Glc}][\text{ATP}]}{1 + \left(\frac{[\text{ATP}]}{K_i}\right)^n}, \quad n = 4.$$

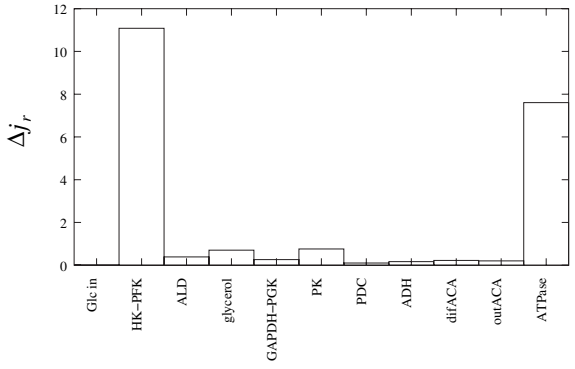

Fig. 5. Relative flux changes in the nine-variable model by Wolf *et al.* [31]. For each reaction, the flux change designates the ratio of the change of flux across a period relative to the minimum flux in the oscillatory cycle. Compare with the experimental data in Fig. 4. Glc in, glucose inflow; HK-PFK, lumped HK, PGI and PFK; glycerol, glycerol branch; GAPDH-PGK, lumped GAPDH, phosphoglycerate kinase, phosphoglycerate mutase and enolase reactions; PDC, pyruvate decarboxylase; difACA, ACA diffusion; outACA, ACA removal (including lactonitrile formation).

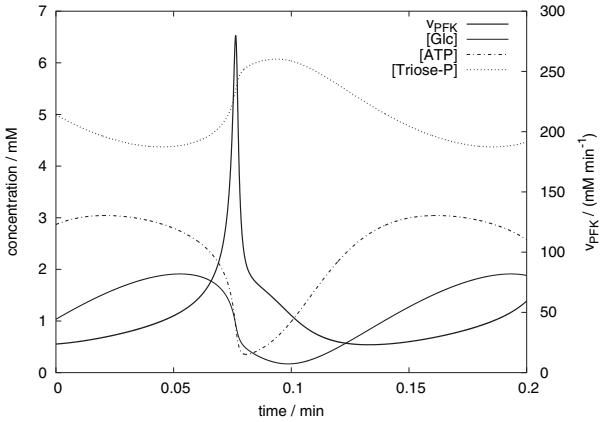

Fig. 6. Relaxation-like oscillations in the nine-variable model by Wolf *et al.* [31]. Triose-P is triose phosphate, i.e. the sum of GAP and DHAP.

The reaction velocity, v depends strongly on the ATP concentration, with the maximum $K_i/\sqrt[4]{3}$ for $n = 4$ and fixed glucose concentration. This is close to the minimum ATP concentration encountered during the oscillations. At the maximum concentration, the reaction velocity, calculated for a fixed glucose concentration, is an order of magnitude lower. Hence, the large variation in PFK flux is due to its regulation by ATP. The ATPase reaction is modelled by simple mass-action kinetics, so the variation in the ATPase velocity reflects a proportional variation in [ATP].

Inspection of the time traces in Fig. 6 reveals that the fast time-scale corresponds to turning on the HK-PFK reaction, whereas the ATPase reaction, the glucose accumulation and the breakdown of triose-phosphates are associated with the slow time scale. When HK-PFK is turned on by low [ATP], a burst of triose phosphates is produced. The lower part of glycolysis produces ATP from the triose phosphates, and the HK-PFK reaction is shut down again. In this state of the reaction system, ATP is consumed by the ATPase reaction, and at some point [ATP] becomes so low that HK-PFK is turned on again. This causes an additional decrease in [ATP] because the HK–PFK reaction consumes ATP itself.

The results of our modified metabolic control analysis are shown in Fig. 7; as is custom, we have only calculated the control exerted by net velocity parameters. The results are in good agreement with those given in Table 6 of [33]. Among the velocity parameters, the amplitude of the oscillations are mainly controlled by glucose inflow followed by ATPase activity. The velocity parameters of the remaining reactions – including PFK – exert only little control. The same conclusions hold for frequency control.

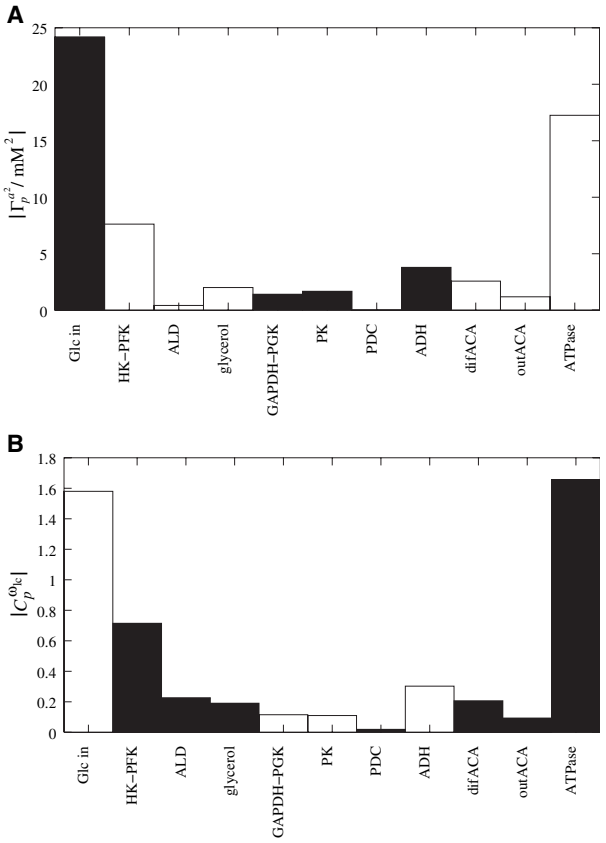

Fig. 7. Modified metabolic control analysis on the limit cycle of the nine-variable model by Wolf *et al.* [31]. (A) $\Gamma_p^{a^2}$ calculations according to Eqn (2). (B) $C_p^{\omega_{Ic}}$ calculations according to the standard definition of control coefficients. For reversible reactions, the coefficients for the forward and the reverse reactions are added in order to reflect the effect of increasing the enzyme concentration. Black bars represent positive values, and white bars represent negative values. Glc in, glucose inflow; HK-PFK, lumped HK, PGI and PFK; glycerol, glycerol branch; GAPDH-PGK, lumped GAPDH, phosphoglycerate kinase, phosphoglycerate mutase and enolase reactions; PDC, pyruvate decarboxylase; difACA, ACA diffusion; outACA, ACA removal (including lactonitrile formation).

These results might seem to contradict the flux-change results, which point to HK-PFK as the central part of the oscillatory mechanism in extracts. A closer inspection of the problem, however, reveals that all of the above results are in mutual agreement. The reason why only a minor fraction of control resides with the 'oscillophore reaction' is due to the on/off nature of the oscillations; it is the regulation of the HK-PFK reaction by ATP that is important for the occurrence of oscillations, not its $V_{max.}$ This notion can be quantified by calculating, for example, $\Gamma_p^{a^2}$ for all parameters in the model and not only the velocity parameters. When we do this, we find that n is the parameter with the largest magnitude of $\Gamma_p^{a^2}$ ($\Gamma_n^{a^2} = 37.8$ mM^2), followed by the other

PFK parameter K_i with $\Gamma^{a^2}_{K_i} = -33.7\text{mM}^2$. These values are directly comparable to those of Fig. 7; the remaining values are $\Gamma^{a^2}_{A_{tot}} = 12.1\text{mM}^2$ and $\Gamma^{a^2}_{N_{tot}} = 2.6\text{mM}^2$.

With this in mind, we can use the on/off switching of PFK to rationalize the results in Fig. 7. Increased ATPase activity shortens the time needed to remove the ATP produced during the previous spike; hence it increases the frequency and decreases the amplitude. Increased glucose inflow results in a higher glucose concentration before the spike and consequently in the production of more ATP, which takes longer time to remove. Therefore, the frequency decreases and the amplitude increases. In other models (e.g. Nielsen *et al.* [14] discussed below) and in experiments [37] the influence of the substrate concentration may outbalance the influence of ATP on PFK activation, resulting in a frequency increase with glucose inflow. The redox state influences the frequency also by changing how much of the triose phosphates are used to produce ATP in the lower part of glycolysis, and how much is used to produce glycerol without ATP production. This effect explains the signs of the frequency control coefficients for ADH, GAPDH and glycerol production.

The seven-variable model in [42] is similar to that analysed here, and our analysis of it leads to the same conclusions (results not shown).

Comparison with the extract model by Nielsen et al.

The yeast extract model of Nielsen *et al.* describes an ATPase-free yeast extract in a CSTR [14]. At the operating point defined by the specific flow $k_0 = 1.1 \times 10^{-2}$ min^{-1} (Fig. 9d in [14]) the model shows relaxation-like oscillations; we will briefly summarize its analysis at this operating point as it shows good agreement with many features of yeast extract oscillations. The relative phases of ATP, ADP, AMP, Pyr and ACA and of F6P, FBP and GAP are in agreement with the experiments reported in [22], whereas the relative phases of phosphoenolpyruvate and $NAD^+/NADH$ are not. The model can also account for the perturbation experiments and bifurcation experiments described in [14]. (The model is analysed as described in that paper, apart from the corrections that the unit of time is in min and $V_{4m} = 10$ mM·min instead of 20 mM·min^{-1}.)

Flux-change analysis of the model (data not shown) shows that PFK has a relative flux-change of 32. This is an order of magnitude larger than any of the other reactions, as expected for an ATPase-free version of Fig. 4. Figure 8 shows the on/off switching of PFK. In this model it is caused mainly by the AMP activation of PFK and, to a smaller extent, by F6P activation and ATP inhibition. In accordance with the flux-change analysis, we find no other reactions exhibiting such an on/off switching.

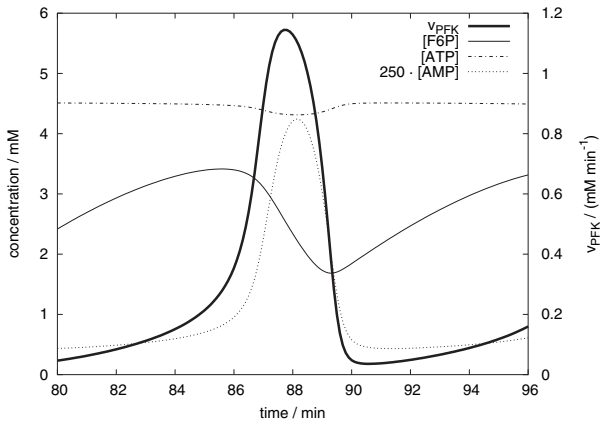

Fig. 8. Relaxation-like oscillations in the extract model by Nielsen *et al.* [14]. Note that [AMP] has been multiplied by a factor of 250 in order to make it visible in the graph. See text for discussions.

Discussion

The mechanism of glycolytic oscillations in intact yeast cells

In the case of intact yeast cells, we are close to a supercritical Hopf bifurcation, and this provides a mathematical framework for our analysis. Both the experimental and model-based analyses by means of polar phase plane plots, and the model-based sensitivity analysis of stability (amplitude) point towards the ATP-ADP-AMP system and the allosteric regulation of PFK as key elements responsible for the occurrence of the instability. The frequency control analysis of the model shows that the frequency of oscillation is controlled by a larger set of control systems, including the redox feedback system. Thus, for intact yeast cells we conclude that frequency control is distributed throughout large parts of the network, whereas the instability of the stationary state originates from PFK and the ATP-ADP-AMP system.

The mechanism of glycolytic oscillations in yeast extracts

In the case of yeast extracts exhibiting relaxation-like oscillations – which is by far the most common type of oscillations observed with yeast extracts – we have identified the fast time-scale as on/off switching of PFK. This finding holds for both experimentally and model-derived data. The phenomenon is caused by AMP activation and/or ATP inhibition; we cannot tell

which of the two is most important as their effects are dynamically equivalent.

In contrast to the case of intact yeast cells, we find that the reactions controlling the frequency of the relaxation oscillations are the same as those controlling the amplitude. This indicates that the yeast extract oscillations are governed entirely by the on/off switching of PFK.

One could argue that this supports the view that PFK is the 'oscillophore' in yeast extracts. The network structure is, however, also important as the on/off switching occurs due to the interplay between the allosteric regulation of PFK and the ATP-ADP-AMP system.

Our analysis of relaxation oscillations is not as sophisticated as that performed on Hopf oscillations, as there is no underlying mathematical frame-work to support the analysis. Lacking this, we cannot judge whether the conclusions obtained for the case of Hopf oscillations in intact yeast cells are also valid for the case of yeast extracts. It is clear from the above discussion, however, that the biochemical components that are of most importance for the oscillations, are the same in the two cases. Probably, the yeast cells are always close to the Hopf bifurcation, simply because the glycolytic flux cannot increase above a value determined by the saturation of the glucose membrane transport system. (This view is consistent with a number of experimental observations, e.g. [18,35–37].)

Biochemical properties derived from Hopf dynamics

Our use of polar phase plane plots to identify the biochemical nature of the activating and inhibitory Hopf modes is the first application of this method. The analysis was performed directly on experimental data without invoking prior knowledge of the reaction network or its regulatory structure. As such, it is a top-down approach well suited for high-throughput methods. The only restriction is that the system should be close to a supercritical Hopf bifurcation. Of particular interest for modelling, the clear biochemical identification of the two Hopf modes provides experimental evidence that a two-dimensional description of glycolysis is sensible not only in terms of abstract Hopf dynamics [19,43], but also in a biochemical formulation where the two variables are energy charge and substrate for either the upper or the lower part of glycolysis.

On the use of sensitivity analysis

When sensitivity analysis of relaxation oscillations is restricted to velocity parameters (i.e. 'enzyme activities'), we find that it will not necessarily be capable of identifying reactions which control the dynamics through their on/off switching. The reason for this is that the important property of such an enzyme is its regulation rather than its maximum velocity.

Summation theorems exist for the frequency control coefficients calculated in metabolic control analysis, but we find here that the coefficients are just as likely to be negative as positive. Therefore, one cannot conclude from determination of one or a few coefficients whether or not they signify a large share of frequency control. Instead, the interesting feature is the relative sizes of the coefficients. This situation differs from that encountered in the common use of metabolic control analysis, where flux-control coefficients are measured. Here, the usual case is that increasing an enzyme activity results in increased flux, and hence flux control coefficients are confined to the interval between zero and one except for a few special cases.

In the neighbourhood of a supercritical Hopf bifurcation, the mathematical framework provided by the Hopf dynamics allows us to relate sensitivity analysis and nonlinear dynamics. This leads to two important findings. One is that control of amplitude is equivalent to control of stability. The other is that the frequency of the oscillations is generally modulated by a larger part of the reaction network than is stability. This is due to the fact that frequency control is the sum of the σ_p' and the σ_p'' contributions (Eqn 3), whereas the control of stability is determined by σ_p' only (Eqn 4). Consequently, it does not make sense to look for an 'oscillophore' in the neighbourhood of a supercritical Hopf bifurcation, if this is thought of as an enzyme controlling both the frequency and amplitude of the oscillations. It is expected that those components controlling stability will generally also control frequency, whereas the opposite is not the case. We have shown that such components can be identified by means of sensitivity analysis.

Cell synchronization

Frequency modulation is of primary importance for the synchronization of the glycolytic oscillations among the individual yeast cells [30,42–44]. In particular, the NAD^+/NADH feedback system will be of primary importance for the cell-synchronization process if the synchronization is mediated by ACA, as has been suggested previously [30,45] (see also [46]). The distributed control of frequency in yeast cells implies that a core model is not well suited for a detailed study of the synchronization problem. Instead, one needs a full-scale model that has been carefully validated

against experimental data. If a simple description is needed for the analysis, then such a model can be reduced to the two-dimensional Hopf form, which gives a quantitatively correct – albeit not 'biochemically formulated' – description of the dynamics [43]. At present, no full-scale model is capable of explaining the synchronization of glycolytic oscillations. The problem is apparently caused by wrong phase-relations between acetaldehyde and the more central parts of the oscillator [43].

Materials and methods

Modified metabolic control analysis of limit-cycle oscillations

Metabolic control analysis is a systematic method for determining control strength. It is a variant of sensitivity analysis where the effects of infinitesimal changes of parameters are quantified. Originally, it was developed for studies of flux control in enzymatic networks, and it has been used previously in the analysis of models describing glycolytic oscillations [32–34]. The control coefficient

$$C_p^X = \frac{\partial X/X}{\partial p/p} = \frac{\partial \ln X}{\partial \ln p} \tag{1}$$

describes the control of a parameter p on a property X. (Strictly speaking, the term 'control coefficient' is only used when p is an enzyme activity; e.g. [47].) We want to discuss the control of the oscillations, so the natural choice of properties is frequency and amplitude of the oscillations.

For the sake of simplicity, it is custom to restrict the analysis to the velocity parameters (i.e. rate constants and $V_{\max}$ parameters) of the rate expressions of the various reactions. In the case of reversible reactions, we just consider the sum of the control coefficients of the forward and reverse reactions. This has the additional advantages that each reaction has exactly one associated control coefficient, and that summation theorems based on time scaling invariance can be applied: increasing all velocity parameters (including the specific flow rate k_0 of the reactor) by a factor f is equivalent to rescaling the time as this changes all time constants of the equations by a factor f^{-1}. Accordingly, stationary state concentrations or the shape and size of a limit cycle will not change. In terms of control coefficients, this means that the control coefficients will sum to one if the system property in question has units including time^{-1}; if it has units not including time, then their sum will be zero.

The control coefficients $C_p^{\omega_{lc}}$ for the frequency on the limit cycle is calculated according to Eqn (1). The calculations for the amplitude of the limit cycle need some consideration; we define the amplitude as the sum of half the peak-to-peak amplitudes of each of the metabolites s: $a = \sum_s a_s$. Furthermore, we choose to calculate:

$$\Gamma_p^{a^2} = \frac{\partial a^2}{\partial p/p} \tag{2}$$

instead of amplitude control coefficients. This is done in order to avoid the singularity, which would otherwise occur at a Hopf bifurcation where the amplitude becomes zero and the slope of the amplitude becomes infinite. Summation theorems can still be derived as indicated above, because we have retained the relative measure $\partial p/p$ for changes in the parameter value p.

Calculations of $C_p^{\omega_{lc}}$ and $\Gamma_p^{a^2}$ were performed with continuation methods using the program CONT [48]. The parameter point chosen for analysis is used as a starting point for short-distance limit-cycle continuations with each of the parameters in the analysis as continuation parameter. Summation theorems were used to check the validity of the calculations or, in some cases, to calculate the control coefficients of a velocity parameter which could otherwise not be calculated due to numerical difficulties. Customised PERL scripts were used to automate this process. This procedure is more efficient and gives better numerical precision than Fourier transform based techniques.

Modified metabolic control analysis at supercritical Hopf bifurcations

We have shown recently that metabolic control analysis – in a form modified to avoid singularities as indicated above – can be related directly to the universal dynamics of systems close to a supercritical Hopf bifurcation [10]. The frequency control coefficient at the bifurcation point becomes:

$$C_p^{\omega_{lc}} = \frac{\mathrm{d}\ln\omega}{\mathrm{d}\ln p} = \frac{1}{\omega_0}\left(\sigma_p'' - \sigma_p'\frac{g''}{g'}\right), \tag{3}$$

and the relative rate of change of stability, which is a scaled measure of the change of the square of the amplitude, is given by:

$$\Gamma_p^{\mathrm{Re}(\lambda)} = \frac{\mathrm{dRe}(\lambda)}{\mathrm{d}\,p/p} = \sigma_p'. \tag{4}$$

In these equations, Re(λ) is the real part of the bifurcating eigenvalue, ω_0 is the frequency of oscillations at the bifurcation point, σ_p' and σ_p'' characterize the rate of change of stability and frequency, respectively, when moving away from the bifurcation point by increasing p. Here, 'stability' refers to the stability of the stationary state which becomes unstable at the bifurcation point. Hence, a positive value of σ_p' indicates that the system moves into the oscillatory region if p is increased. The remaining two parameters g' and g'' characterize the nonlinearity that stabilizes the emerging limit cycle; these parameters are independent of the choice of p.

A measure similar to Eqn (4) has been introduced previously [49]; the present measure has the advantage that the singularity at the bifurcation point is avoided.

For a given Hopf bifurcation point, we use MATHEMATICA (Wolfram Research, Inc., Champaign, IL, USA) to calculate sets of Stuart–Landau parameters (i.e. σ_p', σ_p'', g′ and g″) according to the formulae given in [50]. Each set corresponds to choosing one of the parameters as bifurcation parameter.

Construction of flux-change plots

Flux-change plots are used for identifying reactions exhibiting on/off characteristics. We define the flux change of a reaction as the change in flux across the period of oscillations relative to its minimum flux:

$$\Delta j_r = \frac{j_{\max} - j_{\min}}{j_{\min}}$$

This measure can be obtained from concentration time traces and a subset of in-and effluxes.

By working inwards along each branch of the network, we derive the fluxes through the individual reactions. The data given in [12,22] are sufficient for calculating flux changes for yeast extracts. As only phase and amplitude data are available, we model concentration time traces as sinusoidal oscillations. This approximation softens the edges of the relaxation-like oscillations. Although this underestimates the flux change coefficients, the overall picture is preserved.

The HK flux change is uniquely determined by the substrate injection rate and the glucose time trace. The PGI flux change is given by the HK flux, glycerol production and the G6P time trace. Including the F6P time trace, this also determines the PFK flux-change. The fluxes of the reactions from ADH to GAPDH are determined accordingly. GAPDH, glycerol production and the time traces of GAP and DHAP determine aldolase (ALD) and triosephosphate isomerase (TIM) flux changes. The ATPase flux change is calculated from the fluxes of all ATP or ADP consuming reactions, and the time trace of ATP. The adenylate kinase (AK) flux change is determined trivially from the ATP and ADP time traces.

Analysis by means of polar phase plane plots

Due to universality of the dynamics of systems close to supercritical Hopf bifurcations, it is possible to infer biochemical function from measurements of dynamic properties close to such a bifurcation. It can be shown that, from a dynamic point of view, such systems are composed of only two interacting modes. The properties of these modes are so that one mode activates the other, while the other inhibits the first. The occurrence of the maxima of these two modes is separated in time by one quarter of the period of oscillation (90°), with the activating mode leading the inhibitory mode [10].

We can exploit this understanding of the dynamic system to obtain an interpretation of the biochemical nature of the activating and inhibiting modes. In essence, we do this by mapping the measured phase and amplitude data of the individual metabolites onto the plane of oscillations. For this purpose, we use polar phase plane plots, where the angles reflect the relative phases among the metabolites, and the moduli indicate their relative amplitudes. If a biochemical interpretation of the two Hopf modes is possible, then the datapoints of the metabolites are located along two perpendicular lines, reflecting the 90° phase difference between the Hopf modes. If, on the other hand, no such structure is evident from the plot, then the conclusion is that a simple biochemical interpretation of the two Hopf modes is not possible.

In order to arrive at simpler – and therefore more useful – biochemical interpretations, in some cases we consider the minimum of the concentration oscillation of a metabolite instead of its maximum. As the maximum and the minimum are separated by 180°, this is done by changing the relative phase of that particular metabolite by 180°. If such manipulations have been performed, then this is indicated in the plot. This procedure does not affect the biochemical conclusions. As only the phase differences among the metabolites are considered in the analysis, we can rotate the plots as we please. Theory and details are developed in a separate article [10].

If the data is obtained experimentally, then this kind of analysis has the advantage that no prior knowledge of either the kinetics or the structure of the network is needed. If a model is available, then we use MATHEMATICA to calculate the relative phases and amplitudes from the complex eigenvector of the plane of oscillation. In any case, the method is only applicable close to a supercritical Hopf bifurcation.

Acknowledgements

We thank Barbara Bakker for useful comments and discussions. The work presented here was supported by the Functional Dynamics initiative of the Danish Natural Science Research Council. S.D. acknowledges the financial support provided by the Villum Kann Rasmussen Foundation.

References

1 Ghosh A & Chance B (1964) Oscillations of glycolytic intermediates in yeast cells. *Biochem Biophys Res Commun* **16**, 174–181.

2 Frenkel R (1968) Control of reduced diphosphopyridine nucleotide oscillations in beef heart extracts. II. Oscillations of glycolytic intermediates and adenine nucleotides. *Arch Biochem Biophys* **125**, 157–165.

3 Tornheim K & Lowenstein JM (1974) The purine nucleotide cycle. IV. Interactions with oscillations of the glycolytic pathway in muscle extracts. *J Biol Chem* **249**, 3241–3247.

4 O'Rourke B, Ramza BM & Marban E (1994) Oscillations of membrane current and excitability driven by metabolic oscillations in heart cells. *Science* **265**, 962–966.

5 Nilsson T, Schultz V, Berggren P-O, Corkey BE & Tornheim K (1996) Temporal patterns of changes in ATP/ADP ratio, glucose 6-phosphate and cytoplasmic free Ca^{2+} in glucose-stimulated pancreatic β-cells. *Biochem J* **314**, 91–94.

6 Siegel G, Malmsten MKI, Klüssendorf D & Hofer H-W (1997) Vascular smooth muscle, a multiply feedback-coupled system of high versality, modulation and cell-signaling variability. *Int J Microcirc* **17**, 360–373.

7 Wierschem K & Bertram R (2004) Complex bursting in pancreatic islets: a potential glycolytic mechanism. *J Theor Biol* **228**, 513–521.

8 Winfree A (2000) *The Geometry of Biological Time*. 2nd edn. Springer-Verlag, New York.

9 Richard P (2003) The rhythm of yeast. *FEMS Microbiol Rev* **27**, 547–557.

10 Danø S, Madsen MF & Sørensen PG (2005) Chemical interpretation of oscillatory modes at a Hopf point. *Phys Chem Chem Phys* **7**, 1674–1679.

11 Duysens LNM & Amesz J (1957) Fluorescence spectrophotometry of reduced phosphopyridine nucleotides in intact cells in the near-ultraviolet and visible region. *Biochim Biophys Acta* **24**, 19–26.

12 Boiteux A & Hess B (1973) Control mechanism of glycolytic oscillations. In *Biological and Biochemical Oscillators* (Chance B, Pye EK, Ghosh A & Hess B, eds), pp. 243–252. Academic Press, New York.

13 Nielsen K, Sørensen PG & Hynne F (1997) Chaos in glycolysis. *J Theor Biol* **186**, 303–306.

14 Nielsen K, Sørensen PG, Hynne F & Busse H-G (1998) Sustained oscillations in glycolysis: an experimental and theoretical study of chaotic and complex periodic behavior and of quenching of simple oscillations. *Biophys Chem* **72**, 49–62.

15 Chance B, Williamson G, Lee IY, Mela L, DeVault D, Ghosh A & Pye EK (1973) Synchronization phenomena in oscillations of yeast cells and isolated mitochondria. In *Biological and Biochemical Oscillators* (Chance B, Pye EK, Ghosh A & Hess B, eds), pp. 285–300. Academic Press, New York.

16 von Klitzing L & Betz A (1970) Metabolic control in flow systems. *Arch Mikrobiol* **71**, 220–225.

17 Danø S (1999) *Glycolytic Oscillations in Yeast Cells*. MSc Thesis, University of Copenhagen, Copenhagen.

18 Danø S, Sørensen PG & Hynne F (1999) Sustained oscillations in living cells. *Nature* **402**, 320–322.

19 Hynne F, Danø S & Sørensen PG (2001) Full-scale model of glycolysis in *Saccharomyces cerevisiae*, *Biophys Chem* **94**, 121–163.

20 Higgins J (1964) A chemical mechanism for oscillation of glycolytic intermediates in yeast cells. *Proc Natl Acad Sci USA* **51**, 989–994.

21 Goldbeter A (1996) *Biochemical Oscillations and Cellular Rhythms*. Cambridge University Press, Cambridge.

22 Hess B, Boiteux A & Krüger J (1969) Cooperation of glycolytic enzymes. *Adv Enzyme Regul* **7**, 149–167.

23 Hess B & Boiteux A (1971) Oscillatory phenomena in biochemistry. *Annu Rev Biochem* **40**, 237–258.

24 Boiteux A & Hess B (1974) Oscillations in glycolysis, cellular respiration and communication. *Farad Symp Chem Soc* **9**, 202–214.

25 Hess B (1979) The glycolytic oscillator. *J Exp Biol* **81**, 7–14.

26 Chance B, Holmes W, Higgins J & Connelly C (1958) Localization of interaction sites in multi-component transfer systems – theorems derived from analogies. *Nature* **182**, 1190–1193.

27 Madsen MF (2004) *The Glycolytic Oscillophore*. MSc Thesis, University of Copenhagen, Copenhagen.

28 Sel'kov EE (1968) Self-oscillations in glycolysis. A simple kinetic model. *Eur J Biochem* **4**, 79–86.

29 Goldbeter A & Lefever R (1972) Dissipative structures for an allosteric model. Application to glycolytic oscillations. *Biophys J* **12**, 1302–1315.

30 Richard P, Bakker BM, Teusink B, van Dam K & Westerhoff HV (1996) Acetaldehyde mediates the synchronization of sustained glycolytic oscillations in populations of yeast cells. *Eur J Biochem* **235**, 238–241.

31 Wolf J, Passarge J, Somsen O, Snoep J, Heinrich R & Westerhoff H (2000) Transduction of intracellular and intercellular dynamics in yeast glycolytic oscillations. *Biophys J* **78**, 1145–1153.

32 Bier M, Teusink B, Kholodenko BN & Westerhoff HV (1996) Control analysis of glycolytic oscillations. *Biophys Chem* **62**, 15–24.

33 Reijenga K, Westerhoff H, Kholodenko B & Snoep J (2002) Control analysis for autonomously oscillating biochemical networks. *Biophys J* **82**, 99–108.

34 Teusink B, Bakker B & Westerhoff HV (1996) Control of frequency and amplitude is shared by all enzymes in three models for yeast glycolytic oscillations. *Biochem Biophys Acta* **1275**, 204–212.

35 Becker J-U & Betz A (1972) Membrane transport as controlling pace-maker of glycolysis in *Saccharomyces carlsbergensis,* Biochim. *Biophys Acta* **274**, 584–597.

36 Reijenga K, Snoep J, Diderich J, van Verseveld H, Westerhoff H & Teusink B (2001) Control of glycolytic dynamics by hexose transport in *Saccharomyces cerevisiae*, *Biophys. J* **80**, 626–634.

37 Hess B & Boiteux A (1973) Substrate control of glycolytic oscillations. In *Biological and Biochemical Oscillators* (Chance B, Pye EK, Ghosh A & Hess B, eds), pp. 229–241 Academic Press, New York.
38 Sel'kov E (1975) Stabilization of energy charge, generation of oscillations and multiple steady states in energy metabolism as a result of purely stoichiometric regulation. *Eur J Biochem* **59**, 151–157.
39 Aon MA, Cortassa S, Westerhoff HV, Berden JA, van Spronsen E & van Dam K (1991) Dynamic regulation of yeast glycolytic oscillations by mitochondrial functions. *J Cell Sci* **99**, 325–334.
40 Betz A & Chance B (1965) Phase relationship of glycolytic intermediates in yeast cells with oscillatory metabolic control. *Arch Biochem Biophys* **109**, 585–594.
41 Richard P, Teusink B, Hemker MB, van Dam K & Westerhoff HV (1996) Sustained oscillations in free-energy state and hexose phosphates in yeast. *Yeast* **12**, 731–740.
42 Wolf J & Heinrich R (2000) Effect of cellular interaction on glycolytic oscillations in yeast: a theoretical investigation. *Biochem J* **345**, 321–334.
43 Danø S, Hynne F, De Monte S, d'Ovidio F, Sørensen PG & Westerhoff H (2001) Synchronization of glycolytic oscillations in a yeast cell population. *Faraday Discuss* **120**, 261–276.
44 Ghosh AK, Chance B & Pye EK (1971) Metabolic coupling and synchronization of NADH oscillations in yeast cell populations. *Arch Biochem Biophys* **145**, 319–331.
45 Betz A & Becker JU (1975) Phase dependent phase shifts induced by pyruvate and acetaldehyde in oscillating NADH of yeast cells. *J Interdiscipl Cycle Res* **6**, 167–173.
46 Poulsen A, Lauritsen F & Olsen L (2004) Sustained glycolytic oscillations – no need for cyanide. *FEMS Microbiol Lett* **236**, 261–266.
47 Fell D (1997) *Understanding the Control of Metabolism*. Portland Press, London.
48 Kohout M, Schreiber I & Kubífek M (2002) A computational tool for nonlinear dynamical and bifurcation analysis of chemical engineerig problems. *Comput Chem Eng* **26**, 517–527.
49 Reijenga K (2002) *Dynamic Control of Yeast Glycolysis*. PhD Thesis, Vrije Universiteit Amsterdam, Amsterdam.
50 Ipsen M, Hynne F & Sørensen PG (1998) Systematic derivation of amplitude equations and normal forms for dynamical systems. *Chaos* **8**, 834–852.